

High-power, continuous-wave, mid-infrared optical parametric oscillator based on MgO:sPPLT

S. Chaitanya Kumar^{1,*} and M. Ebrahim-Zadeh^{1,2}

¹*Institut de Ciències Fotòniques (ICFO), Mediterranean Technology Park, 08860 Castelldefels, Barcelona, Spain*

²*Institució Catalana de Recerca i Estudis Avançats (ICREA), Passeig Lluís Companys 23, Barcelona 08010, Spain*

*Corresponding author: chaitanya.suddapalli@icfo.es

Received March 16, 2011; revised June 6, 2011; accepted June 9, 2011;

posted June 10, 2011 (Doc. ID 144371); published July 1, 2011

We report a stable, high-power, cw, mid-IR optical parametric oscillator using MgO-doped stoichiometric periodically poled LiTaO₃ (MgO:sPPLT) pumped by a Yb fiber laser at 1064 nm. The singly resonant oscillator (SRO), based on a 30 mm long crystal, is tunable over 430 nm from 3032 to 3462 nm and can generate as much as 5.5 W of mid-IR output power, with >4 W of over 60% of the tuning range and under reduced thermal effects, enabling room temperature operation. Idler power scaling measurements at ~3.3 μm are compared with an MgO-doped periodically poled LiNbO₃ cw SRO, confirming that MgO:sPPLT is an attractive material for multiwatt mid-IR generation. The idler output at 3299 nm exhibits a peak-to-peak power stability better than 12.8% over 5 h and frequency stability of ~1 GHz, while operating close to room temperature, and has a linewidth of ~0.2 nm, limited by the resolution of the wavemeter. The corresponding signal linewidth at 1570 nm is ~21 MHz. © 2011 Optical Society of America

OCIS codes: 190.4360, 190.4400, 190.4970, 190.2620.

High-power, cw optical parametric oscillators (OPOs) are attractive sources of widely tunable coherent radiation spanning the visible to mid-IR [1], addressing a variety of applications from quantum optics [2] to environmental monitoring [3]. Such sources in the mid-IR are also of interest as first-stage pumps for cw OPOs in tandem, to extend the spectral coverage of these devices beyond the current practical limit of ~4 μm imposed by the onset of absorption in oxide-based nonlinear crystals. To date, practical development of high-power mid-IR cw OPOs has relied mainly on the widely established quasi-phase-matched (QPM) nonlinear material, periodically poled LiNbO₃ (PPLN), providing multiwatt and widely tunable radiation across 1.3–4 μm in the mid-IR [4,5], with as much as 17.5 W of total power at 61% overall extraction efficiency recently achieved in a signal-output-coupled cw OPO based on MgO:PPLN [5]. However, overcoming detrimental thermal effects due to the resonant signal as well as the nonresonant idler at mid-IR wavelengths in PPLN is still a challenge [4,5]. The emergence of new QPM ferroelectric materials, particularly MgO-doped stoichiometric periodically poled LiTaO₃ (MgO:sPPLT), with improved optical and thermal properties [6], has led to important new advances in nonlinear frequency conversion techniques, including single-pass second harmonic generation of IR fiber lasers into the green at unprecedented efficiencies [6,7] and visible-pumped, near-IR OPOs [8]. In spite of a lower effective nonlinear coefficient ($d_{\text{eff}} \sim 9$ pm/V) than PPLN ($d_{\text{eff}} \sim 16$ pm/V), increased resistance to photorefractive damage and higher thermal conductivity along with increased optical damage threshold [9] makes MgO:sPPLT an attractive new alternative to overcome performance limitations of cw PPLN-based OPOs due to thermal effects. Progress in poling technology has also enabled the fabrication of bulk MgO:sPPLT crystals with improved optical quality, longer interaction lengths (30–40 mm) and wide apertures [10], paving the way for the development of practical cw OPOs from visible to the mid-IR in a high-power singly resonant oscillator (SRO) configuration. Moreover, LiTaO₃ is considered to

exhibit lower absorption in the 3–4 μm spectral range than LiNbO₃, making it a potential candidate for high-power mid-IR generation [9].

Earlier work on mid-IR OPOs based on LiTaO₃ pumped at 1064 nm has been in the pulsed regime, including a nanosecond OPO based on sPPLT [10] and a high-energy OPO based on large-aperture MgO:sPPLT pumped by a Q-switched Nd:YAG laser [11]. In these reports, mid-IR idler power scaling has not been studied. To our knowledge, cw OPOs based on MgO:sPPLT pumped at 1064 nm for mid-IR generation have not been previously investigated. It would thus be of great interest to explore the feasibility of using MgO:sPPLT in cw OPOs pumped at 1064 nm for the generation of high-power mid-IR radiation. Here we report a cw OPO based on MgO:sPPLT pumped at 1064 nm, providing high optical powers with wide tuning in the mid-IR. The SRO is tunable over 430 nm with an idler power >4 W over more than 60% of the tuning range and a peak-to-peak power stability of 12.8% over 5 h at 3299 nm. We also investigate mid-IR power scaling of the device and compare its performance with the well-established MgO:PPLN cw SRO pumped at 1064 nm.

The configuration of the cw SRO based on MgO:sPPLT is similar to that in our earlier work [5]. The pump source is a cw, single-frequency Yb fiber laser (IPG Photonics, YLR-30-1064-LP-SF), delivering up to 30 W at 1064 nm in a linearly polarized beam of 4 mm diameter in TEM₀₀ spatial mode ($M^2 < 1.01$), with a linewidth of 89 kHz. The MgO:sPPLT crystal (HC Photonics, Taiwan) is a 30 mm long, 1 mm thick sample with six grating periods from $\Lambda = 29.15$ to 30.65 μm. It is housed in an oven with a temperature stability of ±0.1 °C. The SRO cavity is a symmetric ring, formed by two concave ($r = 100$ mm) and two plane mirrors. All mirrors (LaserOptik, Germany) have high reflectivity ($R > 99\%$) over 1.3–1.9 μm and high transmission ($T > 90\%$) over 2.2–4 μm, ensuring SRO operation. For frequency control, a 500 μm thick uncoated fused silica etalon (free spectral range, FSR ~ 205 GHz) is used at the second cavity waist between the plane mirrors. The pump beam is confocally focused to a beam

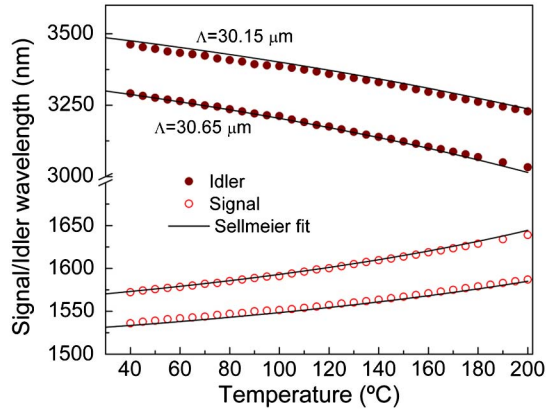


Fig. 1. (Color online) Temperature tuning curves of 1064 nm pumped MgO:sPPLT-based cw SRO.

radius of $48\ \mu\text{m}$ ($\xi \sim 1$) at the center of the crystal. The cavity design ensures optimum overlap of pump and resonant signal at the center of the crystal ($b_p \sim b_s$), with a signal waist radius of $58\ \mu\text{m}$, where b_p , b_s are the confocal parameters of the pump and signal beam, respectively. A dichroic mirror separates the generated output idler from the pump. The total optical length of the cavity including the crystal and the etalon is 575 mm, corresponding to a FSR ~ 522 MHz.

In order to characterize the cw SRO with regard to tunability, we varied the temperature of the MgO:sPPLT crystal from $40\ ^\circ\text{C}$ to $200\ ^\circ\text{C}$. The temperature tuning curves for two grating periods, $\Lambda = 30.65$ and $30.15\ \mu\text{m}$, are shown in Fig. 1. The signal wavelength was monitored using a near-IR spectrum analyzer, while the idler wavelength was measured using a wavelength meter. The solid curves are the theoretical tuning curves calculated from the relevant Sellmeier equations [12]. From Fig. 1, it can be seen that the experimental measurements are in good agreement with the calculated tuning curves.

Figure 2(a) shows the idler power extracted from the MgO:sPPLT cw SRO across the mid-IR tuning range. The data were obtained at an available pump power of 28.5 W at the input to the MgO:sPPLT crystal. Using the two grating periods ($\Lambda = 30.65$, $30.15\ \mu\text{m}$), temperature tuning the SRO from room temperature to $200\ ^\circ\text{C}$ resulted in the generation of idler wavelengths from 3032 to 3462 nm, corresponding to a total tuning range of 430 nm, with a maximum idler power of 5.5 W at 3221 nm and >4 W over more than 60% of the tuning range. The corresponding

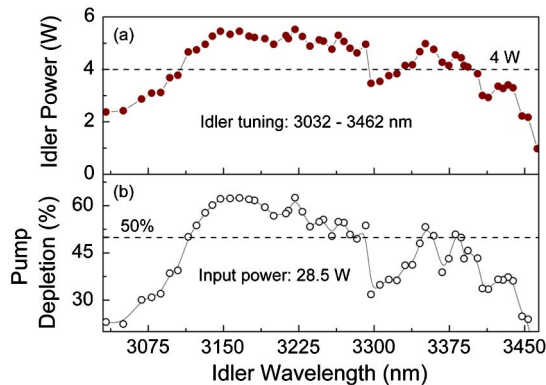


Fig. 2. (Color online) (a) Idler power and (b) pump depletion across the tuning range of MgO:sPPLT cw SRO.

pump depletion across the tuning range is shown in Fig. 2(b), where it can be seen that pump depletion $>50\%$ is achieved over more than 40% of the tuning range. In addition to the idler, a small amount of signal power (few tens of milliwatts) is also obtained as leakage through the plane mirrors of the ring cavity over the entire tuning range. It is interesting to note that, although the thermal load in the nonlinear crystal due to pump, idler, and the high intracavity signal cannot be completely ignored, unlike in the MgO:PPLN cw SRO [5], high-power operation of the MgO:sPPLT cw SRO can be easily achieved at lower temperatures down to $\sim 35\ ^\circ\text{C}$. In contrast, operation of the MgO:PPLN cw SRO at high power is not attainable below $\sim 45\ ^\circ\text{C}$ due to increased thermal effects [5]. The reduced thermal effects in MgO:sPPLT cw SRO can be attributed to intrinsic material properties including higher thermal conductivity ($8.4\ \text{W/m}\cdot\text{K}$), better transmission, and lower circulating intracavity signal power due to lower d_{eff} as compared to MgO:PPLN. Also, the shorter interaction length (30 mm) of the nonlinear crystal results in reduced absorption at pump, signal, and particularly the idler, which become significant at longer wavelengths.

We performed the idler power scaling measurements at different wavelengths across the mid-IR tuning range. Figure 3(a) shows the results obtained at $40\ ^\circ\text{C}$ for a grating period of $\Lambda = 30.65\ \mu\text{m}$ (idler wavelength of 3291 nm). Also included for comparison are the power scaling results for a cw SRO based on a 50 mm long MgO:PPLN at a similar wavelength and operating under the same conditions. Owing to the lower d_{eff} and shorter crystal length (30 mm), the threshold pump power of the MgO:sPPLT cw SRO is recorded to be 17.5 W, while that of the MgO:PPLN cw SRO is only 5.6 W. However, a maximum idler power of 5.2 W is generated for a pump power of 28.1 W at an idler efficiency of 18.5%, with no saturation in the idler power observed. The corresponding maximum idler power generated in the MgO:PPLN cw SRO is 7.6 W for 26.6 W of pump power at an idler efficiency of 28.6%. On the other hand, we also characterized the SRO at a higher temperature of $100\ ^\circ\text{C}$ using the same grating period, corresponding to an idler wavelength of 3212 nm, where we obtained a reduced pump power threshold of 13.2 W and generated as much as 5 W of idler for 29.8 W of pump power, as shown in Fig. 3(b). Also shown in

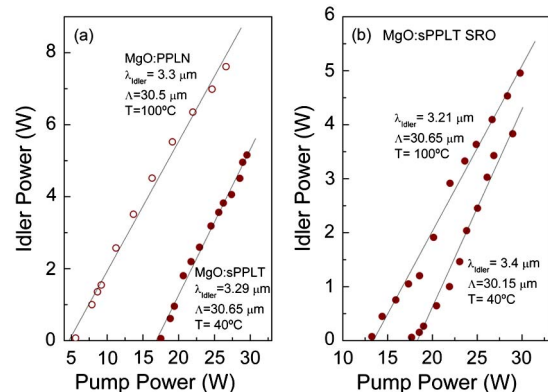


Fig. 3. (Color online) (a) Idler power scaling comparison of MgO:PPLN and MgO:sPPLT cw SROs at $\sim 3.3\ \mu\text{m}$ and (b) idler power scaling of MgO:sPPLT cw SRO at 3.21 and $3.4\ \mu\text{m}$.

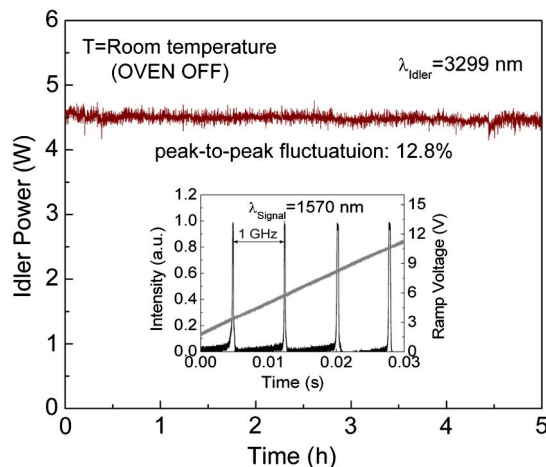


Fig. 4. (Color online) Idler power stability over 5 h at room temperature and (inset) corresponding signal single-frequency spectrum.

Fig. 3(b) is the power scaling at an idler wavelength of 3403 nm, generating 3.8 W of idler for a pump power of 29 W, at a temperature of 40 °C using a grating period of $\Lambda = 30.15 \mu\text{m}$. These measurements confirm that, despite the lower d_{eff} of the material resulting in higher pump threshold, multiwatt idler output powers in the mid-IR can be generated in cw SROs using MgO:sPPLT.

Further, we recorded the idler power stability of the MgO:sPPLT cw SRO close to room temperature at $\sim 35^\circ\text{C}$ (with the oven switched off) corresponding to an idler wavelength of 3299 nm. We obtained a peak-to-peak power stability better than 12.8% over 5 h at an idler power >4.5 W, as shown in Fig. 4. The corresponding signal spectrum at 1570 nm, obtained with the intracavity etalon and recorded using a scanning Fabry–Perot interferometer (FSR = 1 GHz, finesse = 400), is also shown in the inset of Fig. 4, confirming single-frequency operation with an instantaneous linewidth of ~ 21 MHz. Under similar conditions, we also recorded the idler wavelength stability using a wavelength meter (Bristol 721B-IR) with an absolute accuracy of 1 part in 10^6 and a measurement rate of ~ 0.7 Hz.

Figure 5 shows the idler frequency stability recorded over a period of 1 h, confirming a peak-to-peak stability of ~ 1 GHz without any active stabilization. With better thermal isolation and active control, further improvement in the SRO stability is expected. Also shown in the inset of Fig. 5 is the measured idler spectrum centered at 3299 nm with an FWHM linewidth ~ 0.2 nm, limited by the resolution of the wavelength meter. Similar linewidths have been measured at other signal and idler wavelengths across the tuning range. Given the single-frequency nature of the Yb fiber laser pump source with a typical linewidth of 89 KHz, we expect the generated idler wave from the SRO also to be in a single axial mode. However, accurate measurement of idler linewidth requires other methods such as the beat frequency technique.

In conclusion, we have demonstrated a cw SRO based on MgO:sPPLT pumped at 1064 nm, using an Yb fiber

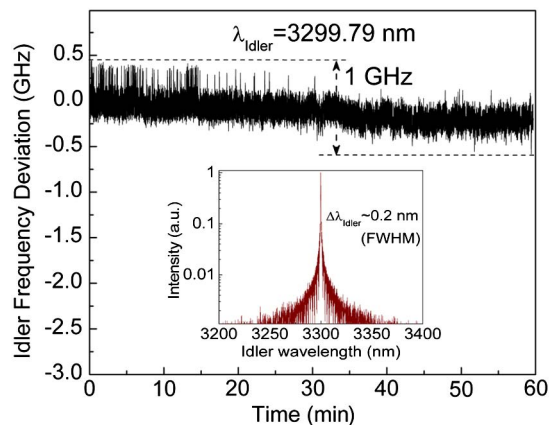


Fig. 5. (Color online) Idler frequency stability over 1 h at room temperature and (inset) corresponding idler spectrum.

laser. The SRO is tunable over 430 nm, generating up to 5.5 W of mid-IR power, with >4 W over 60% of the tuning range, and can be operated close to room temperature, where the signal and the idler linewidth are measured to be ~ 21 MHz and ~ 0.2 nm (limited by the resolution of the wavemeter), respectively. The high output power, low thermal effects, long-term power, and wavelength stability of this cw SRO and the potential for further power scaling confirm that MgO:sPPLT is an attractive nonlinear material for multiwatt cw mid-IR generation.

This research was supported by the Ministry of Science and Innovation, Spain, through grant TEC2009-07991 and the Consolider project, Science and Application of Ultrafast and Ultraintense Lasers (CSD2007-00013). We also acknowledge partial support of this work by the European Office of Aerospace Research and Development (EOARD) through grant FA8655-09-1-3017.

References

1. M. Ebrahim-Zadeh, *Handbook of Optics*, 3rd ed. (Optical Society of America, 2010), Vol. 4, Chap. 17.
2. J. J. Longdell, M. J. Sellars, and N. B. Manson, *Phys. Rev. Lett.* **93**, 130503 (2004).
3. S. M. Cristescu, S. T. Persijn, S. Te Lintel Eckert, and F. J. M. Harren, *Appl. Phys. B* **92**, 343 (2008).
4. A. Henderson and R. Stafford, *Appl. Phys. B* **85**, 181 (2006).
5. S. Chaitanya Kumar, R. Das, G. K. Samanta, and M. Ebrahim-Zadeh, *Appl. Phys. B* **102**, 31 (2010).
6. S. Chaitanya Kumar, G. K. Samanta, and M. Ebrahim-Zadeh, *Opt. Express* **17**, 13711 (2009).
7. G. K. Samanta, S. Chaitanya Kumar, K. Devi, and M. Ebrahim-Zadeh, *Opt. Lett.* **35**, 3513 (2010).
8. G. K. Samanta, G. R. Fayaz, and M. Ebrahim-Zadeh, *Opt. Lett.* **32**, 2623 (2007).
9. N. E. Yu, S. Kurimura, Y. Nomura, M. Nakamura, K. Kitamura, J. Sakuma, Y. Otani, and A. Shiratori, *Appl. Phys. Lett.* **84**, 1662 (2004).
10. H. Ishizuki and T. Taira, *Opt. Express* **18**, 253 (2010).
11. T. Hatanaka, K. Nakamura, T. Taniuchi, H. Ito, Y. Furukawa, and K. Kitamura, *Opt. Lett.* **25**, 651 (2000).
12. A. Bruner, D. Eger, M. B. Oron, P. Blau, M. Katz, and S. Ruschin, *Opt. Lett.* **28**, 194 (2003).